Supporting Information

Guo et al. 10.1073/pnas.1213196109

SI Methods

Constructs and Plasmids. The retroviral miRNA expression library was cloned into the pSCMV vector. pSCMV vector was created by PCR-amplifying a CMV multiple-cloning sites-polyA cassette (with AGAATCTGCTTAGGGTTAGGCGT and TAATGTCGACATCCCCAGCATGCCTGCT) from pcDNA3 (Invitrogen), digesting with NruI and SalI, and inserting into the XhoI and a blunted EcoRI site in the pSuper-puro (Oligoengine) vector. Library cloning was performed by PCR-amplifying human miRNA precursors and ∼150-bp flanking regions on 5′ and 3′ sides from genomic DNA, digesting with indicated enzyme combinations (see Dataset S5 for primers and enzymes), and cloning into BamHI and XhoI sites of pSCMV.

The GFP-containing retroviral vector pMIRWAY-GFP-control and pMIRWAY-GFP-miR-125a was described previously (1, 2). pMIRWAY-GFP-miR-125b-1 was cloned by replacing miR-125a with a PCR amplified fragment (TTCGAATGGGTGAGTTCAGA and TGTGGAATTGCAAGAATAGAAT).

The inducible lentiviral miR-125a plasmid (pFU-tetO-PGK-GFP) was constructed through multiple steps of cloning. In brief, an inducible Gateway destination vector was created by inserting a fragment containing the Gateway cassette (Invitrogen), a PGK promoter and EGFP into the pFU-tetO-Klf4 vector (3) through blunted EcoRI sites. MiR-125a was then cloned into this destination vector through Gateway recombination. A plasmid map is available upon request.

Luciferase reporters were cloned by PCR amplifying the corresponding 3′ UTR from mouse genomic DNA and inserting into psiCheck2 vector (Promega). Primers used include: for *PPP1CA*: TCGCTCGAGCCTCCATGTGCTGCCCTTC and TCGGCGGCCGCGAGAATCCAG CTTTGACCTT; for *PPP2CA*: TCGCTCGAGTGAAAATGTAAACTTGTACA and TCGGCGG CCGCGCCAGAGAGGTTACACAGTG; for DUSP6: TCGCTCGAGAAGGCACCCACCTCT CCTAGC and TCGGCGGCCGCAGCCAAAATAGTTATTTATTA; for *PTPN7*: TCGCTC GAGCCCTCCACCAGCTCATGGG and TCGGCGGCCGCGCATCCAAGAGGTTATTTA; for *PTPN18*: TCGCTCGAGCGAGTGCTGTGCCAGTTATAG and TCGGCGGCCGCTTCTGCC CTGAGAAACTTTTA; for PPME1: TCGCTCGAGTGACCTGCTGTCTACTCCTC and TCG GCGGCCGCTAAAGGTTGGGAGATATTTA; for PPP1R16A: TCGCTCGAGAATGTGA TTCCTCAGTATGG and TCGGCGGCCGCTGGCAAACAGCCTTTATCAAG; for INPP5K: TCGCTCGAGGCCCAGATGGAAGTGAATGA and TCGGCGGCCGCTAAAAGCCATA TTTATAATTAAC.

Mutation of *PTPN18* reporter were performed using PCR-mediated mutagenesis, with the following primer: TCGGCGGCCGCTTCTGGGGACTCAAACTTTTATTTTGAATCAGG. The mutation site is at the end of the 3′UTR, so requiring only one mutation primer.

Luciferase Reporter Assay. Luciferase reporters, including a 3′ UTR-less control reporter, were cotransfected with either a control expression construct or miR-125a expression construct into 293T cells and detected with our published protocol (1, 2). *Renilla* luciferase (under control of 3′ UTR) to firefly luciferase (control luciferase) ratios were used in calculation. Data were first normalized by the mean effect of miR-125a on a 3′ UTR-less control reporter, then normalized by the mean effect of the control expression construct on corresponding UTR reporters.

Cell Culture. BaF3 cells were cultured in RPMI medium with 10% FBS, penicillin, streptomycin, and L-glutamine, supplemented with 3 ng/mL of murine IL-3 (Peprotech). For low IL-3 selection, an IL-3 concentration of 0.05 ng/mL was used. Retrovirus production and infection were performed as described previously (1, 2). Lentivirus production and infection were performed following the RNAi Consortium protocol (4).

MiRNA Functional Screen. The library of miRNA expression vectors was pooled and used to generate pooled viral mixture for infection. Two independent plasmid and viral pools were generated to introduce biological noise. Each viral pool was used twice to independently infect BaF3 cells, resulting in a total of four independently infected cell pools (with two independent infected cell pools for each virus preparation). The amount of virus was titrated to achieve ∼20–30% infection rate. Each infected BaF3 cell population was selected with puromycin and subjected to duplicate and parallel functional screens, resulting in a total of eight replicates for the screen. For each replicate, genomic DNA was harvested at an initial time point after puromycin selection (day 0), whereas a postselection time point was collected after 14 d of low IL-3 selection. Genomic DNA samples were PCR-amplified using primers only present in the vector but not in genomic sequence, with a biotinylated primer (TGTAATACGACTCACTATAGGG) and a nonbiotinylated primer (GATTTAGGTGACACTATAG). PCR products were denatured at 95 °C for 10 min before hybridization. Colored beads (Luminex) coupled with antisense sequences to mature miRNAs were used for detection. Detection probes and hybridization conditions were described previously (2, 5). The detection probes were published (Gene Expression Omnibus GPL10122). After hybridization, beads were washed, reacted with streptavidin-phycoerythrin (Molecular Probes) and detected on a Luminex S100 machine.

Median fluorescence intensity data were used for calculating the barcode relative abundance before and after low IL-3 selection, after the data were normalized using probes with the least variable ranks (the criteria for invariant probes are: the SD of the rank of probe intensity to be less than 7 among all samples, and the maximum intensity of the probe across samples to be at least 500). After invariant probe normalization, data below 16 (log2 of 4) were set to 16 to avoid low signal noise to generate false positives. To identify candidate miRNAs, normalized barcode data (Dataset S1) were log2-transformed and subjected to pair-wise t test (by comparing after selection to before selection of the same biological samples, using excel function) to determine nominal P values based on student's t distribution. A pair-wise t test was performed because the overall probe-level pair-wise differences (after log2 transformation), comparing after selection to before selection, had a distribution similar to normal distribution. False-discovery rate were then calculated based on the Benjamini–Hochberg method. In addition, we performed permutation test to assess P value. This process was performed by permuting the sample labels, and using paired t test statistics as a scoring measure, for a total of 10,000 times. False-discovery rates were calculated based on permutation P values as well (Dataset S1). Candidate miRNA probes in Fig. S1*A* were determined that satisfy two criteria: (*i*) false-discovery rate (based on P value from Student t test) < 0.15 and (*ii*) at least one sample has log2 barcode value >7 (to avoid noise).

Bone Marrow Transplantation. Lethal irradiation was delivered by a cesium irradiator for a total of 9 Gy. Hematopoietic stem and progenitor cells (HSPC) viral transduction and transplantation was performed as described previously (1). Briefly, donor mice were primed with 150 mg/kg 5-fluorouracil (5-FU), and after 4 d, bone marrow cells were harvested for overnight viral transduction in x-vivo15 medium (BioWhittaker) supplemented with 100 ng/mL of SCF, 50 ng/mL of Flt3L, 50 ng/mL of TPO, and 50 ng/mL of IL-3 (all from Peprotech). On the following day, 1–2 × 10^6 viable cells were injected into irradiated hosts via tail vein. Unless otherwise specified, all mice used were wild-type C57Bl6/J purchased from Jackson Laboratory. For experiments with the inducible i125a, Rosa26-rtTA mice (Jackson Laboratory) were used as donors. Doxycycline (Dox) was supplied in drinking water at 1 mg/mL and sweetened with 1% (wt/vol) sucrose (all from Sigma). For transplanting, a low dose of i125a-transduced HSPCs, FACS-sorted Lin-$Sca1^+Kit^+$ cells were used for viral transduction. After overnight infection, cultures containing derivatives from ~800 starting $Lin^-Sca1^+Kit^+$ cells were transplanted into wild-type recipients with 500,000 whole bone marrow cells for radio-protection. For other experiments with i125a, the 5-FU–based protocol was used.

Animal Maintenance and Histology Analysis. All mouse work was approved by the Yale University Institutional Animal Care and Use Committee according to federal and institutional policies and regulations. All animals were maintained by the Yale Animal Resource Center. Histological sections and staining were performed by the Mouse Research Pathology Core at Yale University. Complete blood count was performed on a Hemavet 950FS machine. Blood smears and cytospun slides were stained using standard May-Grünwald solutions (Sigma). Images were acquired using an Olympus BX51 upright microscope.

Quantitative PCR and RNA Analysis. Quantitative PCR for miRNA expression was measured using the miScript PCR system (Qiagen). Total RNA was prepared using TriZol (Invitrogen) and assayed by specific primers for miR-125a, or miR-125b and RNU6B (normalization control). Expression data were normalized using RNU6B as a control.

PTPN18 RNA levels were measured. Erythroid myeloid lymphoid cells were transduced with a control vector, or miR-125a. Transduced cells were analyzed with Affymetrix Mouse 430 2.0 arrays. Data were normalized by robust multiarray algorithm.

Flow Cytometry. FACS analyses were performed using a BD FACS Calibur or LSRII analyzer. For peripheral blood analyses, 40 µL of whole blood were treated with BD FACS lysing solution (BD Biosciences), washed and stained in antibody mixtures. For bone marrow, cells were obtained from femurs and tibiae by flushing or crushing and stained in antibody mixtures. All antibodies were from BD Biosciences or eBiosciences. Analysis of p-Tyr was performed as we have described previously (1) with an antibody from Cell Signaling.

Colony Formation Assay. Base methylcellulose without cytokines (M3234; Stemcell Technologies) was used following the manufacturer's instructions. Next, 25,000 bone marrow mononuclear cells were plated in six-well plates in the presence of various concentration of IL-3 or GM-CSF. On day 10 after plating, the numbers of colonies containing more than 30 cells were scored and photographed using an Olympus IX51 inverted microscope.

Statistics. All P values were calculated using Student t test, unless specified otherwise.

1. Guo S, et al. (2010) MicroRNA miR-125a controls hematopoietic stem cell number. *Proc Natl Acad Sci USA* 107:14229–14234.
2. Lu J, et al. (2008) MicroRNA-mediated control of cell fate in megakaryocyte-erythrocyte progenitors. *Dev Cell* 14:843–853.
3. Maherali N, et al. (2008) A high-efficiency system for the generation and study of human induced pluripotent stem cells. *Cell Stem Cell* 3:340–345.
4. Moffat J, et al. (2006) A lentiviral RNAi library for human and mouse genes applied to an arrayed viral high-content screen. *Cell* 124:1283–1298.
5. Lu J, et al. (2005) MicroRNA expression profiles classify human cancers. *Nature* 435:834–838.

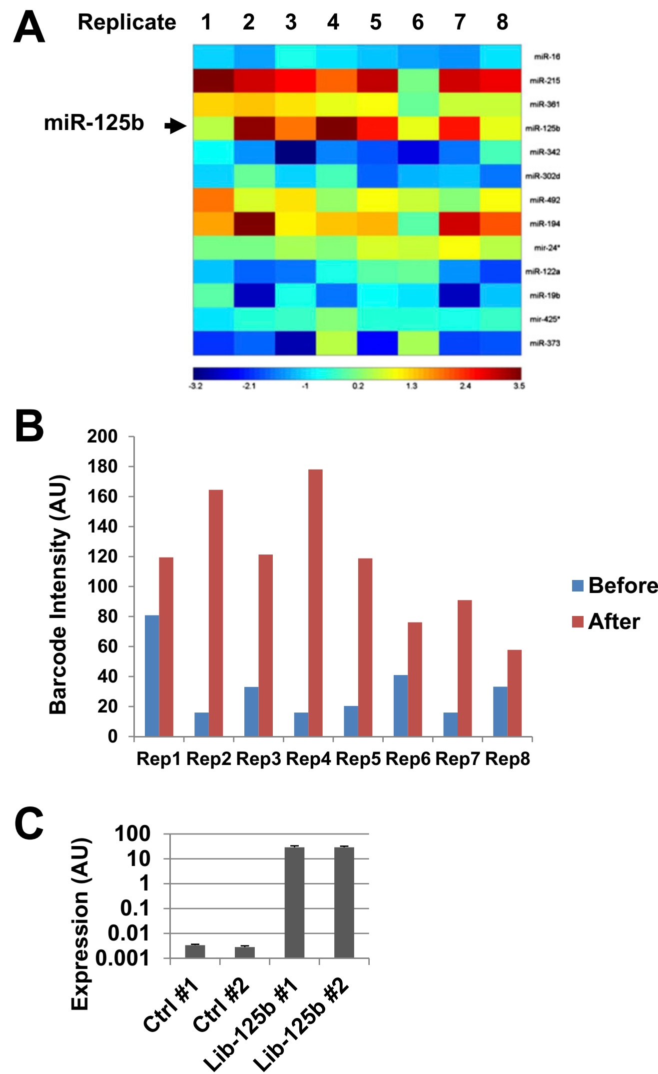

Fig. S1. A functional genomic screen identifies miR-125b as a hit. (*A*) A heatmap of detected barcodes that display false-discovery rates (based on *P* values from Student *t* test) < 0.15. Data displayed reflect the log2 value of the ratio between barcode values after and before low IL-3 selection. Arrow points to the miR-125b barcode. Red color means enriched after low IL-3 selection. Blue color means depleted after low IL-3 selection. Rows stand for miRNA barcodes and columns stand for experimental replicates. (*B*) The barcode intensities for miR-125b are shown for a total of eight replicates (Rep) before and after low IL-3 selection. (*C*) The level of miR-125b overexpression was measured in BaF3 cells. The vector for miR-125b in the screen, or a miRNA-less control vector, was used to transduce BaF3 cells in biological duplicates. Expression of miR-125b was measured by quantitative RT-PCR. Error bars represent SDs of quantitative RT-PCR assays.

Fig. S2. Leukocytosis and monocytosis in miR-125a recipient animals. (*A*) Peripheral blood white blood cell count (WBC) and monocyte count (MO) were followed in miR-125a recipient animals using a HEMAVET 950FS machine. A representative cohort is shown. (*B*) Representative blood smears of control-vector (Ctrl) or miR-125a transplant recipients. (Magnification: 40×.) Note the prevalence of reticulocytes (blue-gray colored RBCs) indicative of stress erythropoiesis. (*C*) Progressive anemia is shown with RBC count from control of 125a recipients, at 2 mo (mo) or 4 mo posttransplantation. A representative cohort is shown.

A

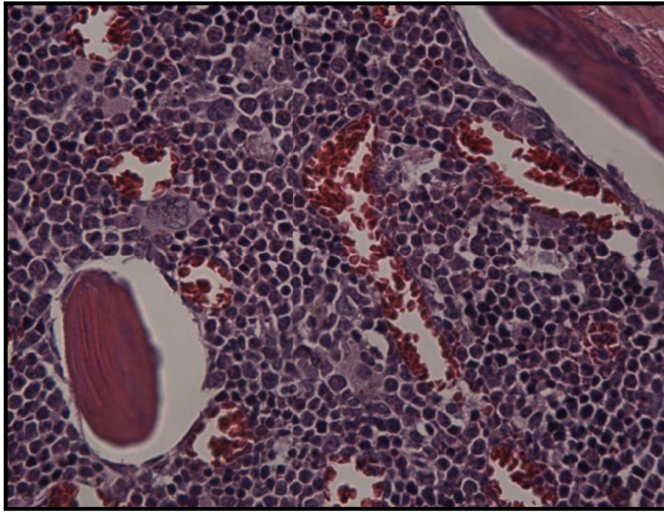

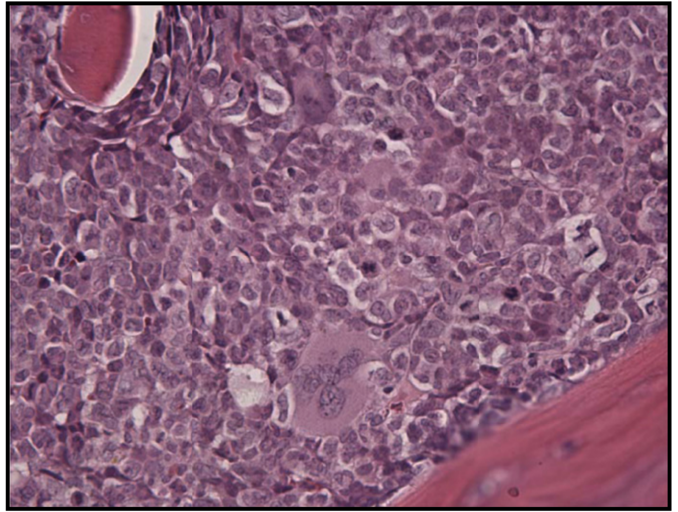

B

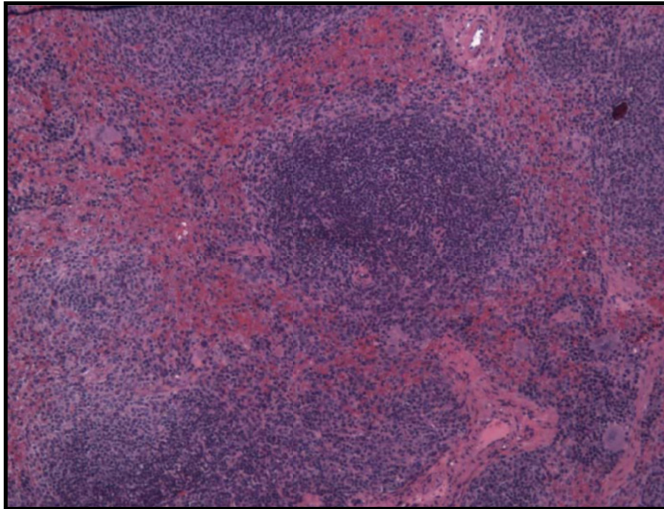

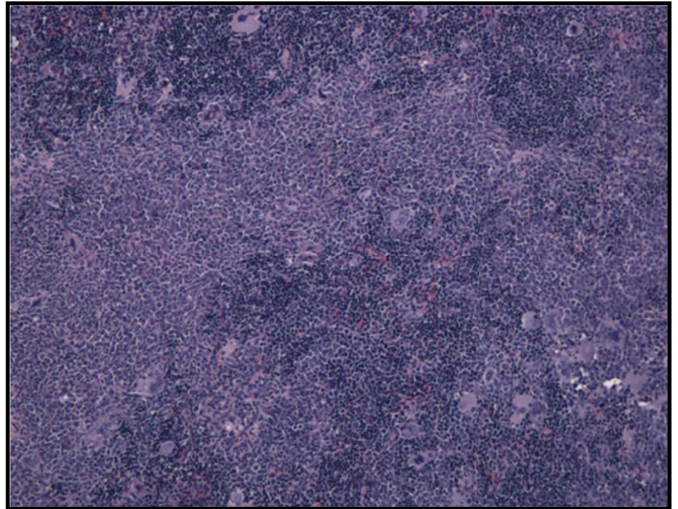

Fig. S3. miR-125a recipients display disruption of normal histology in bone marrow and spleen. Bone marrow (*A*, 40× magnification) and spleen (*B*, 10× magnification) of control or miR-125a transplant recipients. Representative images are shown. Note that the bone marrow of miR-125a recipient is largely occupied by myeloid cells, and that there is prominent effacement in the miR-125a recipient spleen with disruption of regular white and red pulp structures.

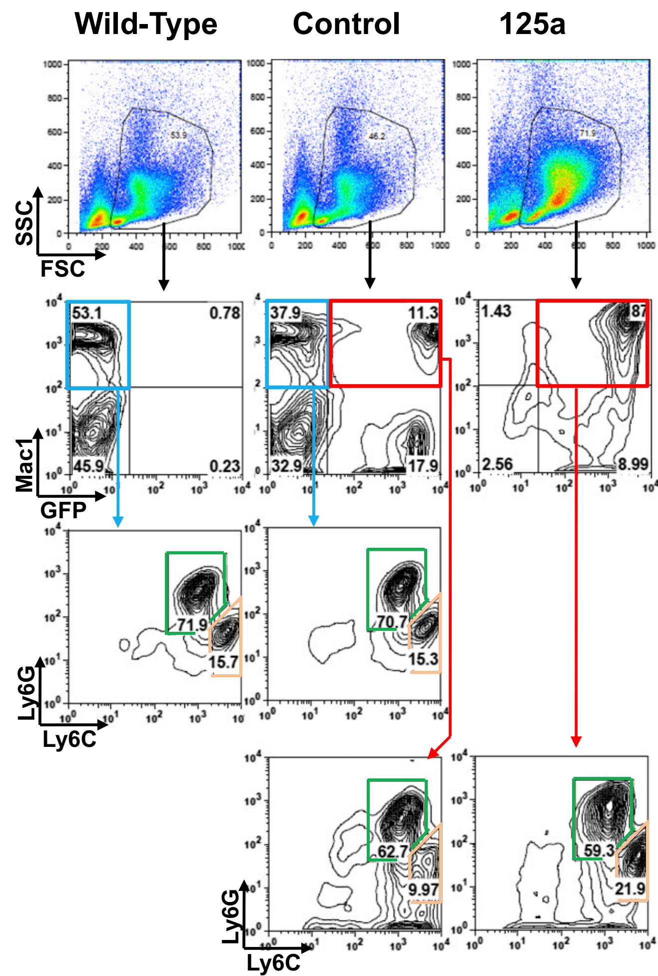

Fig. S4. MiR-125a transplant recipients showed expansion of bone marrow granulocytic and monocytic cells. Bone marrow cells from wild-type, control-vector transplant recipient, or miR-125a recipient were analyzed by flow cytometry. Representative plots are shown. Note that the expanded myeloid population ($GFP^{+}Mac1^{+}$) in miR-125a recipient contains both granulocytic cells ($Ly6G^{hi}Ly6C^{low}$) and monocytic cells ($Ly6G^{low}Ly6C^{hi}$).

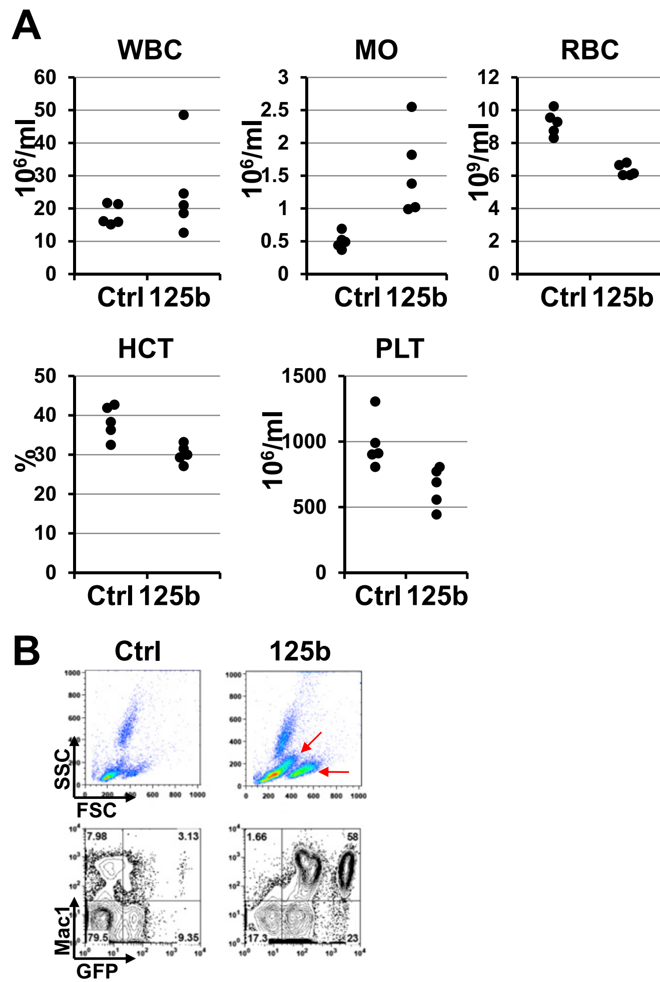

Fig. S5. MiR-125b transplant recipient mice display similar MPN phenotypes as miR-125a recipients. (*A*) Complete blood counts of control (ctrl) or miR-125b transplant recipients 5 mo posttransplantation. HCT, hematocrit; MO, monocyte; PLT, platelet; RBC, red blood cell; WBC, white blood cell. (*B*) Flow cytometry analysis of peripheral blood. Note the increase of the characteristic $FSC^{hi}SSC^{low}$ populations (red arrows) and $GFP^{+}Mac1^{+}$ population in 125b recipients.

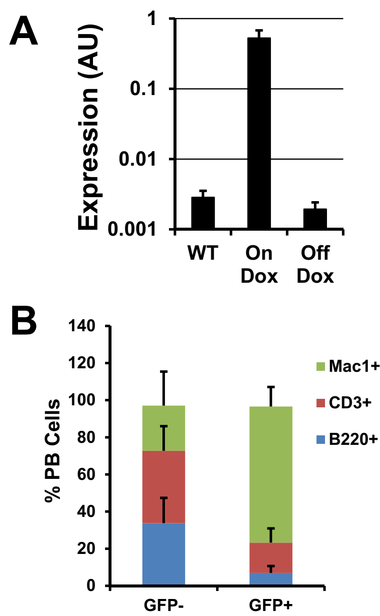

Fig. S6. Analyses of the i125a model. (*A*) Inducible miR-125a expression in i125a mice. The expression level of miR-125a was measured by quantitative PCR in the bone marrow cells from wild-type, or i125a recipient mice on Dox or switched off Dox. Expression level was normalized by that of RNU6B and displayed in arbitrary units (AU). Error bars represent SD of the quantitative PCR assay. (*B*) Peripheral lineage bias in i125a recipients. Myeloid, B- and T-cell fractions in peripheral blood (PB) were determined by flow-cytometry using indicated markers. Transduced (GFP^+) and nontransduced (GFP^-) populations are shown. n = 11. Error bars represent SD.

Fig. S7. Rare anemic conditions improve after Dox removal in i125a transplant recipients. (*A*) RBC and hematocrit level in i125a mice that have been maintained on Dox. Each line represents one individual animal over time. The horizontal red line indicates the anemic cutoff. Note that a small number of recipients developed anemia after 4 mo. A representative cohort is shown. (*B*) For the few animals that developed anemia, RBC and hematocrit were measured before Dox and after Dox removal (2 wk). The data on these animals were pooled from two independent cohorts. (*C*) For the other i125a recipients that did not qualify as anemia, RBC parameters were followed with time. Red arrow indicates the time of Dox removal. Note that the parameters increased for three of four recipients, but the one animal without significant improvement had high red cell parameters before Dox removal. Blue lines indicate anemic cutoff.

A

On Dox

Off Dox

B

Fig. S8. Peripheral blood smears of i125a mice and bone marrow colony formation in the constitutive model. (*A*) Blood smears were prepared for a representative i125a recipient, either on Dox or 2 wk off dox. (Magnification: 40×.) (*B*) MiR-125a (constitutive expression) transplant recipient bone marrow cells gave rise to colonies in the absence of IL-3 or GM-CSF. Bone marrow cells from a miR-125a recipient were seeded for colony-formation assay with no IL-3 or GM-CSF. Picture was taken with 10× lens after 10 d in culture. A representative colony is shown.

A

Spleen

Control Recipient

i125a 1st Round Dox

i125a 2nd Round Dox #2

i125a 2nd Round Dox #3

B

Lung

Control Recipient

i125a 2nd Round Dox #1

Fig. S9. Complex outcomes in i125a mice exposed with a second round of induction. (*A*) Severe spleen stromal collapse in two i125a mice exposed with a second round of Dox (*Lower*). Arrows point to acellular areas with collapsed stroma. Mouse ID numbers correspond to those in Dataset S4. Note that the presence of white and red pulps in control recipient spleen, the spleen effacement in i125a mice on first round of Dox which is similar to that seen in the constitutive model (Fig. S3), and lack of normal structures in mice on second round of Dox. (*B*) Severe hematopoietic infiltration into the lung in one i125a mouse on second round of Dox. A control construct recipient is also shown. All sections were stained with H&E and images acquired with a 4× objective lens. Note that the long black streaks on the spleen sections are sectioning artifacts.

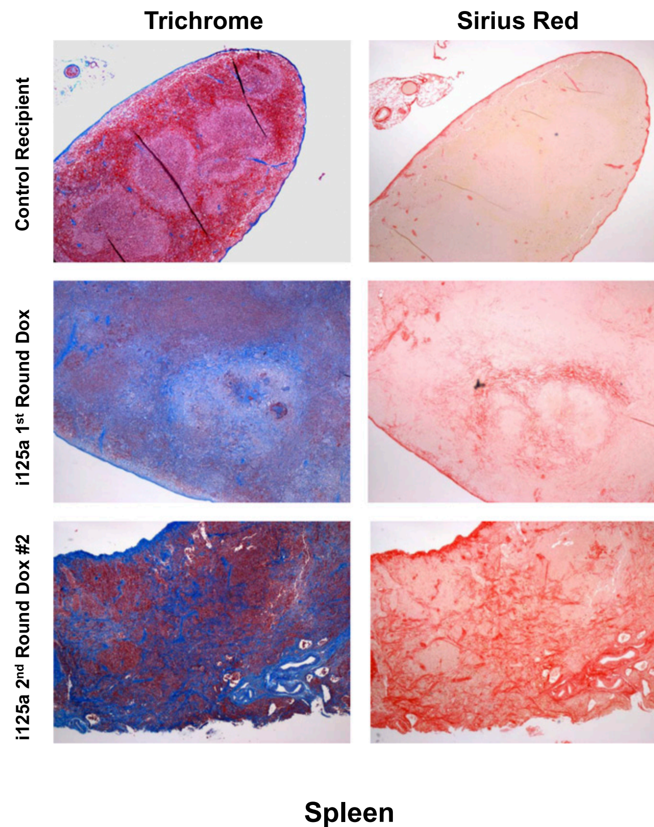

Fig. S10. Fibrotic lesions in the collapsed stroma of spleen. Spleen sections from control recipient, i125a mouse on first round of Dox, and i125a mouse #2 on second round of Dox (mouse number correspond to that in Dataset S4) were stained with trichrome and Sirus red, which produce blue and red colored signals on collagen fibers respectively. Note the strong blue and red stainings in i125a mouse #2 on second round of Dox. All images were acquired with a 4× objective lens. Another recipient, i125a mouse #3 on second round of Dox had similar strong fibrotic staining. Note that the long black streaks on the spleen sections are sectioning artifacts.

Other Supporting Information Files

Dataset S1 (XLSX)
Dataset S2 (XLSX)
Dataset S3 (XLSX)
Dataset S4 (XLSX)
Dataset S5 (XLSX)